Bilal, M., and Jackson, S. D. (2017) Ethanol steam reforming over Pt/Al2O3 and Rh/Al2O3 catalysts: the effect of impurities on selectivity and catalyst deactivation. Applied Catalysis A: General, 529, pp. 98-107. (doi:10.1016/j.apcata.2016.10.020)

This is the author's final accepted version.

There may be differences between this version and the published version. You are advised to consult the publisher's version if you wish to cite from it.

http://eprints.gla.ac.uk/130423/

Deposited on: 20 October 2016

Enlighten – Research publications by members of the University of Glasgow
http://eprints.gla.ac.uk

Ethanol steam reforming over Pt/Al_2O_3 and Rh/Al_2O_3 catalysts: the effect of impurities on selectivity and catalyst deactivation.

Muhammad Bilal† and S. David Jackson*

Centre for Catalysis Research, WestCHEM, School of Chemistry, University of Glasgow, Glasgow G12 8QQ, Scotland, UK

e-mail: david.jackson@glasgow.ac.uk

* author to whom all correspondence should be addressed

† now at Department of Chemistry, Kohat University of Science and Technology, Kohat, Pakistan.

Abstract

Bioethanol contains different types of organic impurities which can have a significant influence on the catalytic performance during steam reforming of bioethanol. Different C_3 functional group impurities were added individually to the pure ethanol to investigate the influence of different functional groups on the ethanol steam reforming reaction over 0.2 % Pt/Al_2O_3 and 0.2 % Rh/Al_2O_3 catalysts at 773 K. It was established that the catalytic behaviour of both of the catalysts is significantly influenced by the different impurities. The addition of 1 mol % C_3 alcohols (1-propanol and isopropyl alcohol) significantly decreased the conversion of ethanol and increased the rate of catalyst deactivation. This deactivation of the catalyst in the presence of C_3 alcohols was attributed to high olefin formation and incomplete decomposition of the C_3 alcohols, which deposited over the catalysts as coke. Propanal, propylamine and acetone addition to the water/ethanol mixture resulted in rapid metal deactivation and a loss of steam reforming activity over the Pt/alumina although ethanol decomposition continued. In contrast the Rh/alumina did not lose all steam reforming activity when acetone and propylamine were added as impurities. On both the catalysts alcoholic impurities produced a large number of carbon nanotubes (CNTs).

Keywords: ethanol; steam reforming; impurities; Pt/Al_2O_3; Rh/Al_2O_3

1. Introduction

In the past, wood and coal were the primary sources of energy. However, in the 20th century after the discovery of petroleum, the primary source of energy for transportation became petroleum based [1]. As petroleum and natural gas are non-renewable feedstocks with a limited lifespan, there is a need to solve the energy problem of the future. Several technologies have been developed and touted, e.g. wind, wave, solar, photovoltaic and others, as potential solutions [2, 3]. Among the most promising near term technologies are those based on fuel cells [4]. The use of fuel cells for electric power generation in automobiles has immense potential as they exhibit high efficiency, are environmentally friendly and have operational benefits when compared to conventional technologies [5]. Hydrogen, which is the most common fuel for fuel cells, is currently commercially produced on the large scale principally by steam reforming of natural gas, with lesser roles for partial oxidation of heavy oil residues and partial oxidation of coal [6, 7]. However the formation of hydrogen from biomass derived sources is promising future technology because the raw material used is renewable. Among the different renewable sources, a keen interest has been taken in bioethanol in the last few years as bioethanol feedstock is environmentally benign. Also, a higher hydrogen yield per mole can be obtained from steam reforming when ethanol is used as a reactant compared to methanol or methane. Moreover ethanol has no negative effect on the human body during handling [8]. According to Bion *et al.* [9] comparison of the Gibbs free energy of the steam reforming of ethanol (47.7 kJ.mol^{-1}) and ethane (107.7 kJ.mol^{-1}) gave the idea that

ethanol is more feasible than ethane. The main products for steam reforming of ethanol are H_2, CO and CO_2.

$$C_2H_5OH + 3H_2O \rightarrow 2CO_2 + 6H_2 \quad (1)$$

$$C_2H_5OH + H_2O \rightarrow 2CO + 4H_2 \quad (2)$$

However, other reactions such as dehydration, dehydrogenation, cracking, water gas shift reaction and methanation reactions can be influenced by catalyst precursors and support [10]. The ethanol dehydration reaction, which often takes place on the acidic sites of the support, produces ethene and is a primary source of coke which deactivates the catalyst [11].

Bioethanol can be obtained from biomass by a fermentation process which contains about 20 vol% of ethanol with water as the major component [12]. Biomass such as sugar cane, sugar beet, wheat, straw, potatoes and other organic waste can be converted to ethanol by the help of yeast. In Brazil bioethanol is mainly produced from sugar cane whilst in the USA it is produced from corn [9].

Most of the investigations concerning ethanol steam reforming have been performed using pure ethanol and distilled water mixtures [5, 11, 13], however, steam reforming of crude ethanol differs from that of the pure ethanol by the fact that the impurities present in the crude ethanol feed have a significant influence on hydrogen formation as well as affecting catalyst activity and stability [9]. The impurities found in bioethanol are

variable and depend upon the source of the bioethanol [14] but typically higher alcohols such as propanol, 2-propanol (isopropyl alcohol, IPA) and mixed C-4 alcohols, aldehydes, esters (typically ethyl acetate), ketones such as acetone and nitrogen bases [14]. A few studies have been performed using crude bioethanol or model bioethanol. Among them Alkande *et al*. [15] firstly used direct crude bioethanol for steam reforming, which was obtained from the fermentation of starch of wheat and found that initially the catalyst activity was high and then decreased with time on stream. Recently Epron *et al.* [9] studied the effect of various impurities on the steam reforming of bioethanol over $Rh/MgAl_2O_4$ by using model raw bioethanol feeds and reported that addition of a diethylamine increased the ethanol conversion whilst butanol and ethyl acetate had a poisoning effect and decreased the ethanol conversion. The effect of different alcohols have also been investigated and it was found that higher alcohols (both linear or branch) significantly decreased the conversion of ethanol and hydrogen yield [16].

The work in this paper is part of a study into the effect of different impurities on the bioethanol steam reforming reactions using precious metal catalysts. A previous paper investigated Ru/alumina [17]. In this paper, alumina supported rhodium and platinum catalysts were investigated using a model bioethanol containing 1 mol. % C_3 impurities such as 1-propanol, 2-propanol (IPA), propanal, acetone and propylamine. By choosing a common three carbon chain backbone for all the impurities, the effect of the functional group could be isolated. A medium pressure was used to mimic an industrial application. As well as following the reaction over an extended period, post reaction characterisation

of the spent catalysts was carried out using a range of techniques to investigate the cause of catalyst deactivation during the steam reforming of ethanol.

2. Experimental

The catalysts used were a 0.2 % Pt/Al_2O_3 and Rh/Al_2O_3 prepared via incipient wetness impregnation. The alumina was determined by x-ray diffraction (XRD) analysis to be a mixture of γ- and δ-alumina phases. The metal salts used were $Rh(NO_3)_3$ and H_2PtCl_6. After drying, the catalysts were calcined at 723 K for 4 h. The BET surface area of the calcined catalysts was 104±3 m^2g^{-1}, while the metal dispersions were determined by hydrogen chemisorption as 4 % for Rh/alumina and 18 % for Pt/alumina. The catalysts were crushed to particle sizes between 600 to 425 μm before use in steam reforming of ethanol using a series of impurities.

Ethanol (AnalaR Normapur, 99.99%), acetone (Fisher Scientific, 99.99%), IPA (Sigma Aldrich, 99.5%), 1-propanol (Alfa Aesar, 99.0%), propylamine (Sigma Aldrich, 99.0%) and propanal (Sigma Aldrich, 97.0%) were all used without further purification.

A continuous-flow, high-pressure, microreactor with a 3/16 inch internal diameter and 18.5 inch long glass-lined stainless steel reactor tube was used for ethanol steam reforming reactions. Prior to reaction, catalysts (0.25 g, 0.51 cm^3) were reduced *in-situ* at 873 K for 2 hours using hydrogen gas at a flow rate of 50 ml min^{-1}. The hydrogen was purged from the system with argon and the temperature decreased to the reaction

temperature (773 K) simultaneously the total pressure in the apparatus was increased to 20 barg. The water-ethanol mixture was set to deliver an H_2O:C_2H_5OH molar ratio of 5:1 in the gas phase. A 1 mol. % impurity (relative to ethanol) was added to the water-ethanol mixture. This modified ethanol-water mixture was introduced to the reactor through a vaporizer set at a temperature of 773 K. The gas flow rate of the steam/ethanol was set at 416 ml min^{-1}, which was generated by pumping the liquids through a Gilson pump at a rate of 0.412 ml min^{-1}. The argon gas flow rate was set at 10 ml min^{-1} giving an overall gas flow rate of 426 ml min^{-1} at STP with a H_2O:C_2H_5OH:Ar ratio of 34.7:6.9:1. The gas hourly space velocity (GHSV, 25560 cm^3 h^{-1}/0.51 cm^3) was calculated to be 50,000 h^{-1}. Once all the reaction parameters had been fixed, analysis was begun by flowing reactants from vaporizer to reactor. The eluant from the reactor tube in gaseous form entered a knockout pot where high boiling point products were liquefied and collected and analysed by a Trace GC-2000 Series using a Zebron column and FID detector. The temperature of the knockout pot was kept at 273 K. The gaseous products were analysed by an on-line Varian GC 3400 using a TCD detector and a carboxen^{Tm}1010 plot column. Each reaction was on stream for 100 h at 773 K. Mass balance in the system was ~100 %. The extent of carbon deposition as a function of the feed was < 1 %.

The amounts and nature of carbon deposited on the catalyst were determined by analysing post reaction catalyst samples using analytical techniques such as BET, powder XRD, Raman spectroscopy, scanning electron microscopy (SEM) and thermogravimetric

analysis coupled to differential scanning calorimetry (TGA-DSC) connected to a mass spectrometer for evolved gas analysis.

BET surface areas and pore volume of pre- and post-reaction catalysts were measured using a Micromeritics Gemini III 2375 Surface Area Analyser. Prior to analysis, between 0.04-0.05g of catalyst were placed into a vial and purged under a flow of N_2 (30ml min^{-1}) over night at 383 K to remove moisture and any physisorbed gases from the catalyst sample. Powder X-ray diffraction patterns of pre and post reaction samples were obtained using a Siemens D 5000 X-ray Diffractometer (40kV, 40mA, monochromatic). The scanning range was $5^o \leq 2\ \theta \leq 85^o$ with a scanning rate of 10 seconds per step and a step size of 0.02°. Raman spectra of post reaction catalysts were obtained with a Horiba Jobin Yvon LabRAM High Resolution spectrometer. A 532.17nm line of a coherent Kimmon IK series He-Cd laser was used as the excitation source for the laser. Laser light was focused for 10 seconds using a 50x objective lens and grating of 600. The scattered light was collected in a backscattering configuration and was detected using nitrogen cooled charge-coupled detector. A scanning range of 100 and 4100 cm^{-1} was used. SEM images of the post reaction catalysts were obtained using a Philips XL30 Environmental SEM. The sample was irradiated with a beam of electrons, this was followed by changing magnification and focusing for increasing resolution of the catalyst surface. TPO was carried out on post reaction samples using a combined TGA/DSC SDT Q600 thermal Analyser connected to an ESS Mass Spectrometer for evolved gas analysis. Each sample was heated from room temperature to 1000^{o}C using a heating ramp of 5^{o}C min^{-1} under 2% O_2/Argon gas at a flow rate of 100 ml min^{-1}.

The calculations used in this paper are summarised here.

Ethanol conversion was calculated as follow:

% Conversion

= [mmoles of ethanol in – mmoles of ethanol out]/ [mmoles of ethanol in]*100

The selectivity of different products were calculated by using the following formula

% Selectivity = [mmoles of product X out]/ [mmoles of all the products]*100

3. Results

In order to determine how different functional groups affect the ability of the catalysts to perform ethanol steam reforming (ESR), five different organic functional groups coupled to a basic C_3 structure (1-propanol, 2-propanol (IPA), propanal, propylamine and acetone) were tested by adding to the water/ethanol reactant mixture, in a 1% molar ratio with respect to the ethanol content.

An initial experiment was performed using the alumina support. In a previous study [18] it was shown that alumina does not catalyse steam reforming of ethanol but instead catalyses ethanol decomposition and the water gas shift (WGS) reaction. The results from the reaction, over the alumina support, of ethanol with 1-propanol and propyl amine as added impurities have been previously reported [17] and show similar behaviour in that the product distributions confirm that the only reactions occurring are ethanol

decomposition and WGS. The selectivity of the reaction with propylamine and 1-propanol additives can be described at 100 h by the following reactions:

$$3C_2H_5OH \rightarrow 3CO + 3CH_4 + 3H_2$$

$$2CO + 2H_2O \rightarrow 2CO_2 + 2H_2$$

Overall: $3C_2H_5OH + 2H_2O \rightarrow CO + 3CH_4 + 5H_2 + 2CO_2$

3.1. Rh/alumina.

The addition of 1 mol.% impurities of 1-propanol, IPA, propanal, acetone and propylamine to the water/ethanol mixture had a noticeable effect on ethanol conversion over the Rh/Al_2O_3 catalyst at 773 K and 20 barg pressure (Fig. 1). The conversion of ethanol was higher in all the reactions containing an impurity than the pure ethanol reaction up to 25 h time-on-stream (TOS). However after 25 hrs TOS, a rapid decrease in ethanol conversion took place when 1-propanol and IPA were the impurities, such that these systems lost over 50 % of their activity. In contrast the reactions where propanal and acetone had been added showed higher ethanol conversion than in the absence of an impurity for the whole TOS: although both had started to show deactivation. The reaction with propylamine as the impurity showed enhanced reactivity over the pure ethanol up to 75 h TOS, however in the last 25 h the activity dropped to just below that found with the pure ethanol.

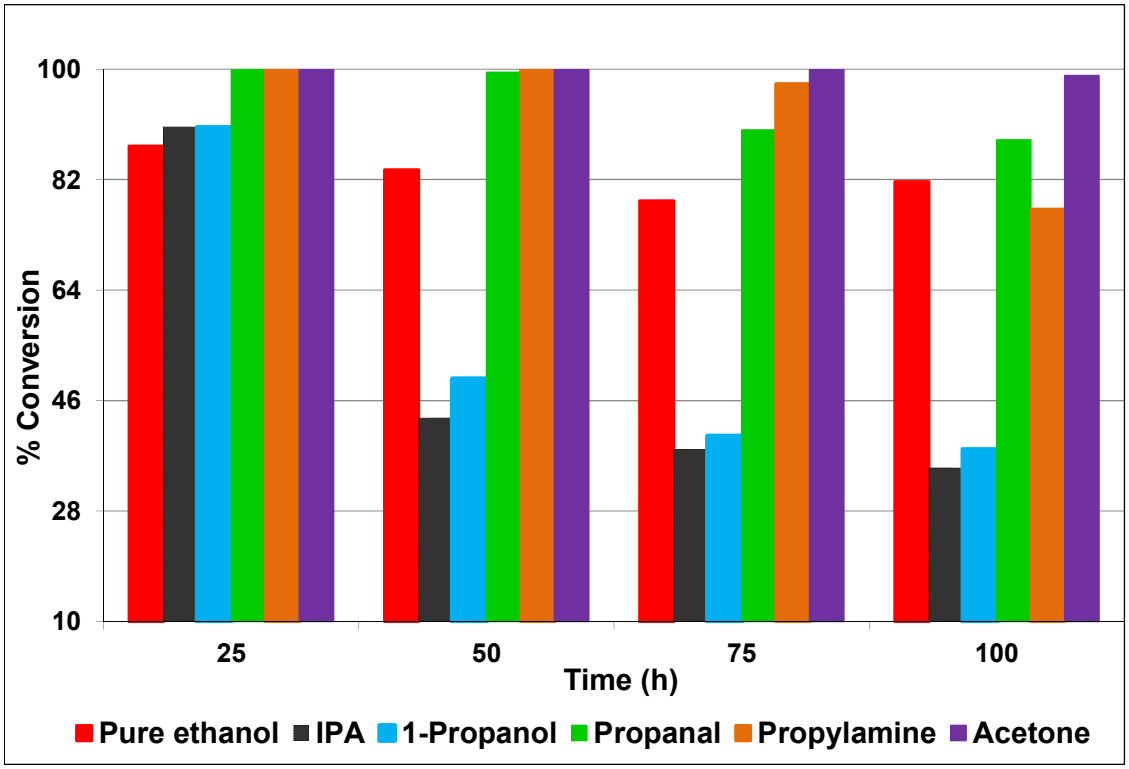

Figure 1. Conversion of ethanol over Rh/Al_2O_3 during reaction containing different impurities. Conditions: 773 K, 20 barg, 5:1 water:ethanol, 1 % impurity

The only significant product condensed in the liquid phase was acetaldehyde (Fig. 2). For the pure system the yield (acetaldehyde produced/ethanol fed) starts at ~10 % but decreases with time on stream, in contrast the opposite is seen with experiments containing propylamine and acetone impurities where the yield increased with time on stream. Diethyl ether was also detected but only at low levels typically < 0.5 % yield.

The dry gas selectivities are reported in Table 1, where two different groups are visible. The reaction with pure ethanol and those with IPA and 1-propanol show high hydrogen selectivity, moderate ethene selectivity and low methane selectivity, whereas the

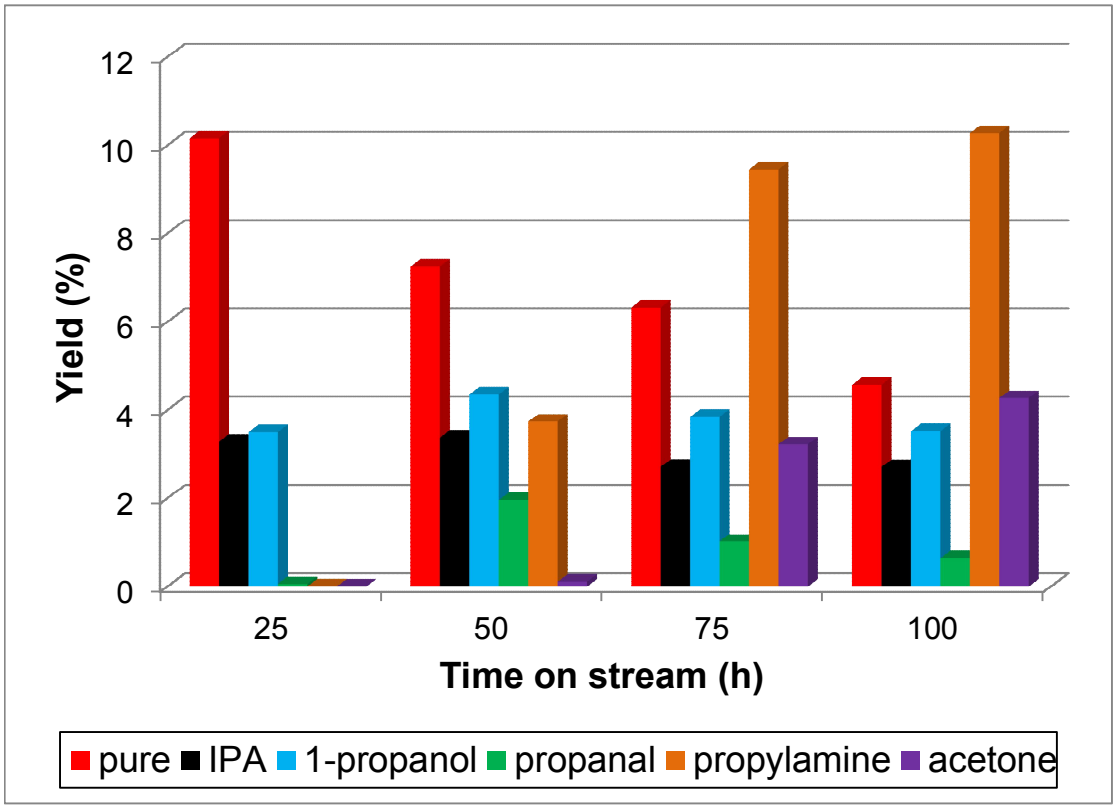

Figure 2. Yield of acetaldehyde over Rh/alumina with time on stream.

Table 1. Dry gas selectivities at 100 h TOS over Rh/alumina at 773 K.

Impurity	**Molar dry gas selectivity (%)**					
	H_2	**C_2H_4**	**CO_2**	**CO**	**CH_4**	**C_2H_6**
No impurity	64	16	8	4	6	2
IPA	64	14	13	2	5	1
1-Propanol	54	27	10	2	5	1
Propanal	45	0	19	7	29	0
Propylamine	47	1	20	3	28	0
Acetone	44	4	19	5	27	0

experiments with propanal, propylamine and acetone exhibit much higher methane selectivity, lower hydrogen selectivity and very low ethene selectivity.

After use the catalysts were characterised by Raman spectroscopy, BET analysis and TGA. The Raman spectra revealed two major bands at around 1325 cm^{-1} and 1586 cm^{-1} that can be assigned to the D and G of graphitic carbon (Fig. 3). Other bands were detected at ~2600 – 3100 cm^{-1}. The intensity ratio of the I_D/I_G is also reported in table 2 along with the BET surface areas. The surface areas decreased significantly as did the pore volume.

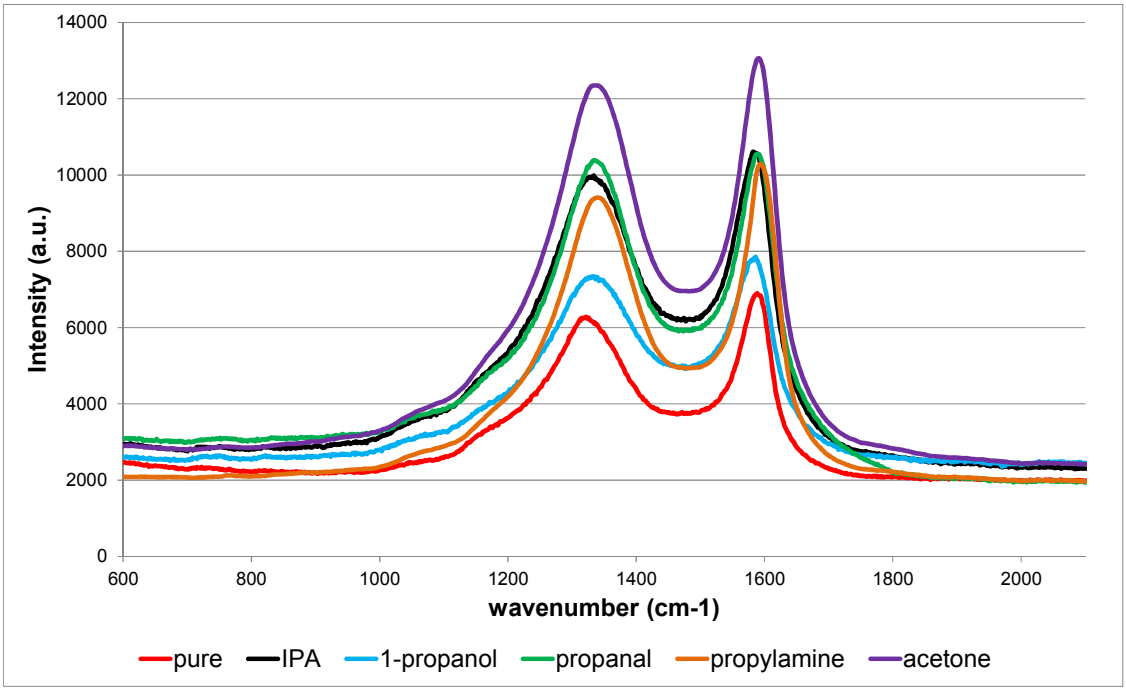

Figure 3. Raman spectra of Rh/alumina catalysts after use in ESR.

To determine the nature of coke deposition on the catalysts, the spent catalysts of the pure ethanol and all the impurities reactions were analysed by TGA/DSC/MS under flow of 2% O_2/Ar gas which is shown in Figure 4. The sole carbon containing species evolved during the TGA was carbon dioxide which was determined by mass spectrometry. In addition to this mass, fragments with m/z values of 2, 18, 26, 27, 28, 29, 31, 58, 59, 60 and 78 were monitored, however only trace amounts of water were detected in some samples whilst no prominent peaks were observed for other masses. Hence the weight

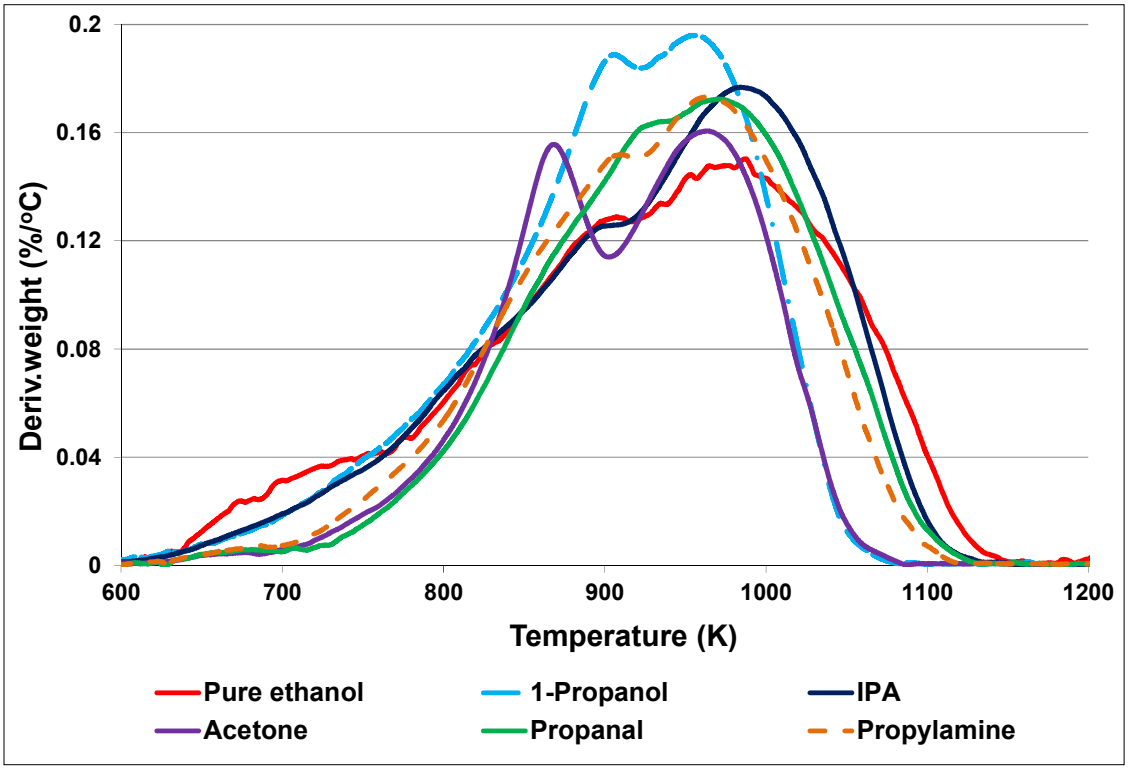

Figure 4. TGA analysis of spent ESR Rh/alumina catalysts in 2 % O_2/Ar. Weight loss represents loss of carbon dioxide.

loss can be assigned to the removal of carbon and the profile for the carbon dioxide evolution matches the derivative weight profile. All of the profiles show two weight loss

events a main one around 975 – 1000 K, the other at around 900 – 925 K except for the spent catalyst used with acetone as the impurity, where the low temperature weight loss occurs as a very clear separate event at 863 K. The weight loss is reported in table 2.

Table 2. BET surface area, % weight loss and Raman band ratios over Rh/Al_2O_3 for reactions with different impurities.

Impurity	BET Surface area (m^2g^{-1})	Pore volume (cm^3g^{-1})	Weight loss in TPO (%)	(I_D/I_G)
Reduced@600	101	0.46	-	-
No impurity	47	0.04	41	0.91
IPA	39	0.03	41	0.94
1-propanol	39	0.07	39	0.93
Propanal	32	0.08	37	0.98
Propylamine	31	0.07	37	0.91
Acetone	45	0.11	31	0.94

To study the catalyst morphology, all of the spent catalysts were analysed by SEM. The SEM images of Rh/Al_2O_3 after use (Fig. 5) show that all samples (pure ethanol and all the impurities) gave small size carbon nanotubes CNTs.

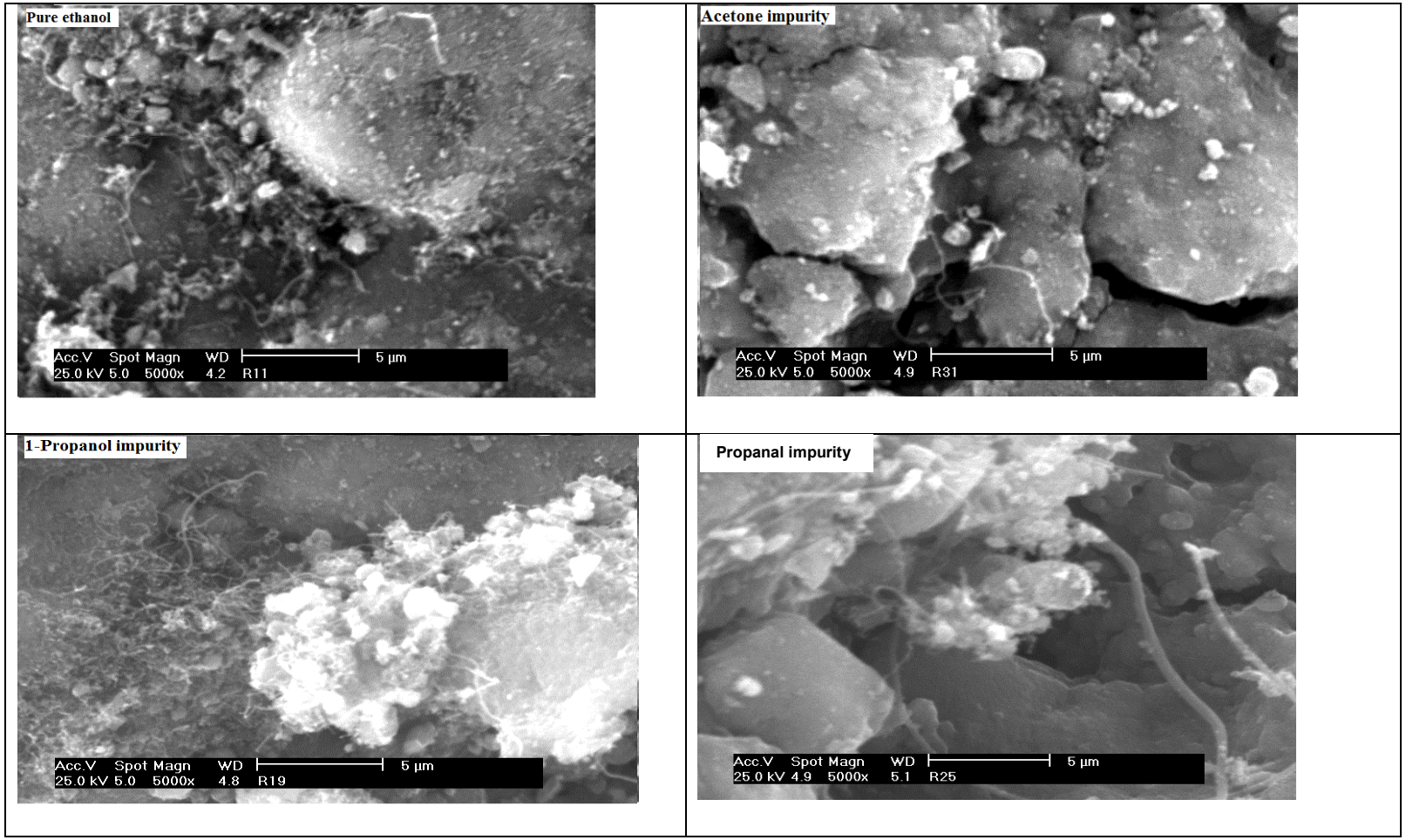

Figure 5. SEM images for post reaction Rh/Al_2O_3 used with pure ethanol, 1-propanol, propanal and acetone impurity reactions.

3.2. Pt/alumina.

The addition of 1 mol.% impurities of 1-propanol, IPA, propanal, acetone and propylamine to the water/ethanol mixture had a noticeable effect on ethanol conversion over the Pt/Al_2O_3 catalyst at 773 K and 20 barg pressure (Fig. 6).

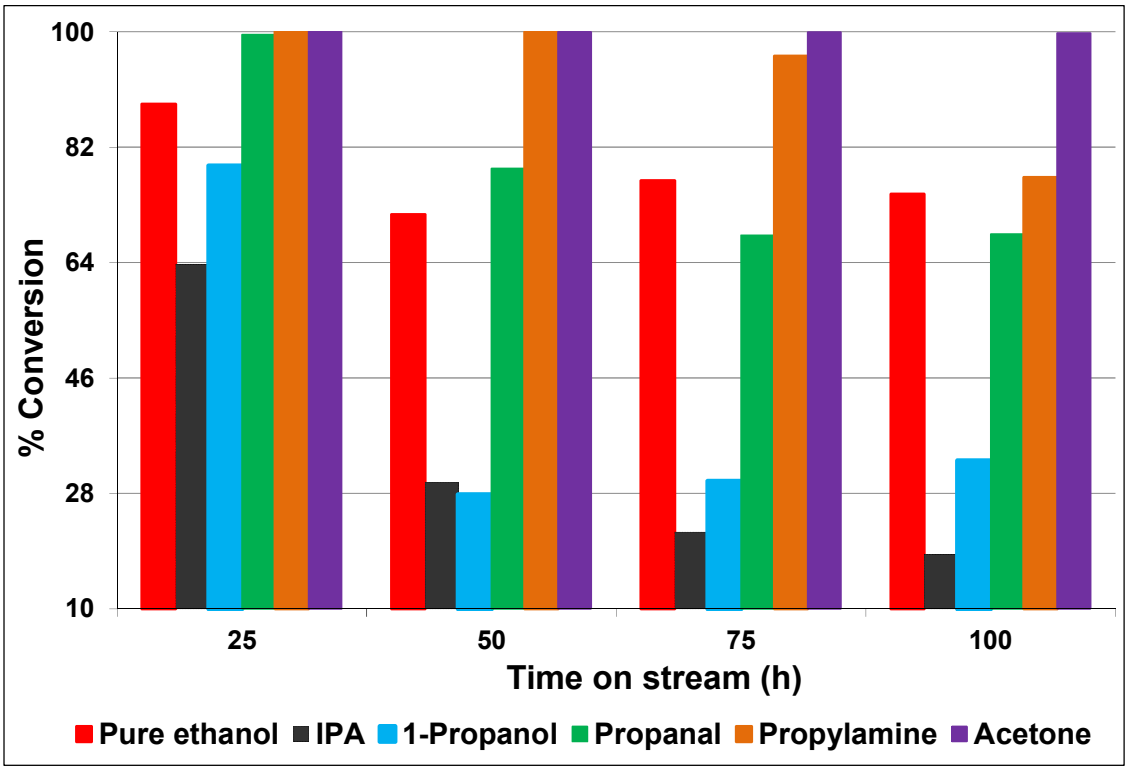

Figure 6. Conversion of ethanol over Pt/Al_2O_3 during reaction containing different impurities. Conditions: 773 K, 20 barg, 5:1 water:ethanol, 1 % impurity.

Both IPA and 1-propanol caused significant deactivation even after just 25 h on stream. By 100 h the conversion of ethanol, when 1 % IPA was present, had been reduced to around 20 % in contrast to ~70 % in the absence of an impurity. 1-propanol was also

highly deleterious reducing the conversion to ~30 % after 100 h TOS. Propanal and propylamine reduced the conversion to levels similar to that for pure ethanol after 100 h even though initially they gave higher conversion. No deactivation was observed at all when acetone was added as an impurity.

The main product condensed as a liquid from the reaction was acetaldehyde and a difference in behaviour is seen between the pure ethanol reaction, where the yield of acetaldehyde decreases with TOS and the reactions with propylamine and acetone as impurities, where acetaldehyde yield increases with TOS (Fig. 7).

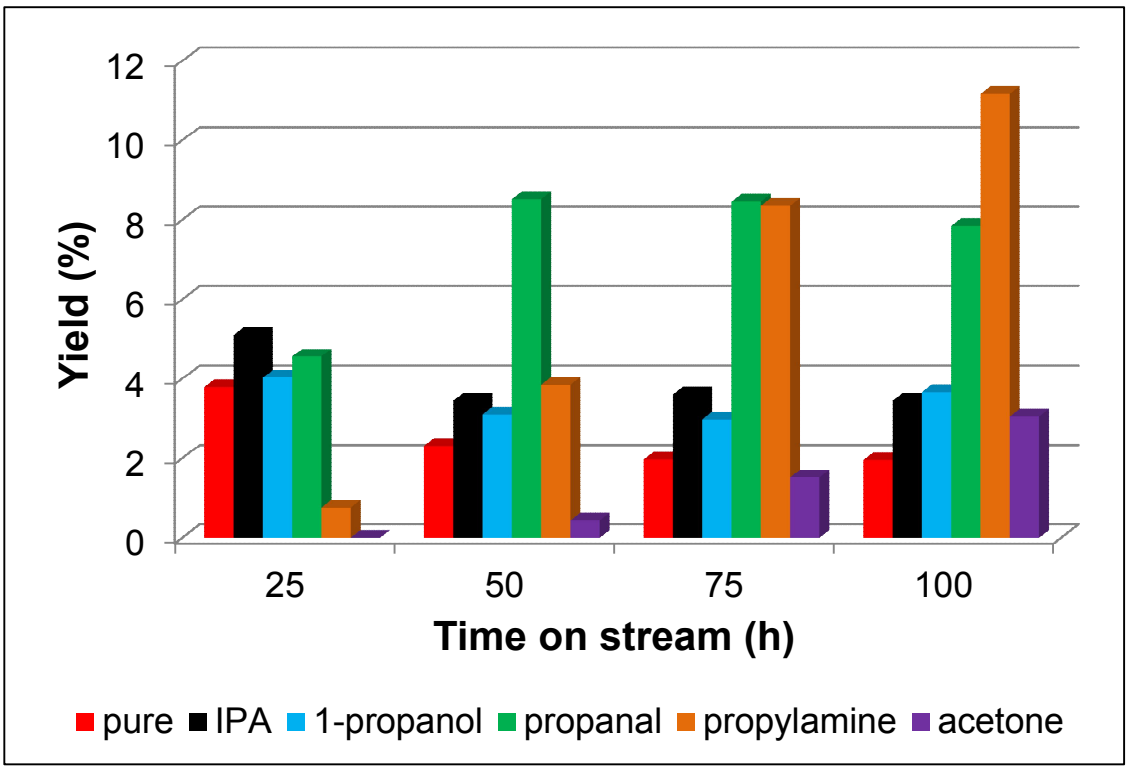

Figure 7. Yield of acetaldehyde over Pt/alumina with time on stream.

Over the Pt/alumina catalyst acetone was also seen as a condensed liquid product. The behaviour matches that of acetaldehyde with the yield decreasing for pure ethanol and for the experiments with IPA and 1-propanol in the feed, whereas the acetone yield increases when propanal, propylamine and acetone impurities are present. The highest yield (~ 3 %) was observed in the propylamine containing reaction.

The dry gas selectivities are reported in Table 3, where again two different groups are visible. The reaction with pure ethanol and those with IPA and 1-propanol show moderate ethene selectivity and low methane selectivity, whereas the experiments with propanal, propylamine and acetone exhibit much higher methane selectivity and very low ethene selectivity.

Table 3. Dry gas selectivities at 100 h TOS over Pt/alumina at 773 K.

Impurity	**Molar dry gas selectivity (%)**					
	H_2	**C_2H_4**	**CO_2**	**CO**	**CH_4**	**C_2H_6**
No impurity	53	24	9	2	7	4
IPA	59	17	12	1	8	3
1-Propanol	62	15	11	1	8	2
Propanal	52	0	20	4	24	0
Propylamine	51	1	19	5	24	0
Acetone	45	4	17	8	26	0

After use the catalysts were characterised by Raman spectroscopy, BET analysis and TGA. The Raman spectra revealed two major bands at around 1340 cm^{-1} and 1590 cm^{-1} that can be assigned to the D and G of graphitic carbon (Fig. 8). Other bands were detected at ~2600 – 3100 cm^{-1} consistent with C-H stretching vibrations. The intensity ratio of the I_D/I_G is also reported in table 4 along with the BET surface areas. The surface areas decreased significantly as did the pore volume.

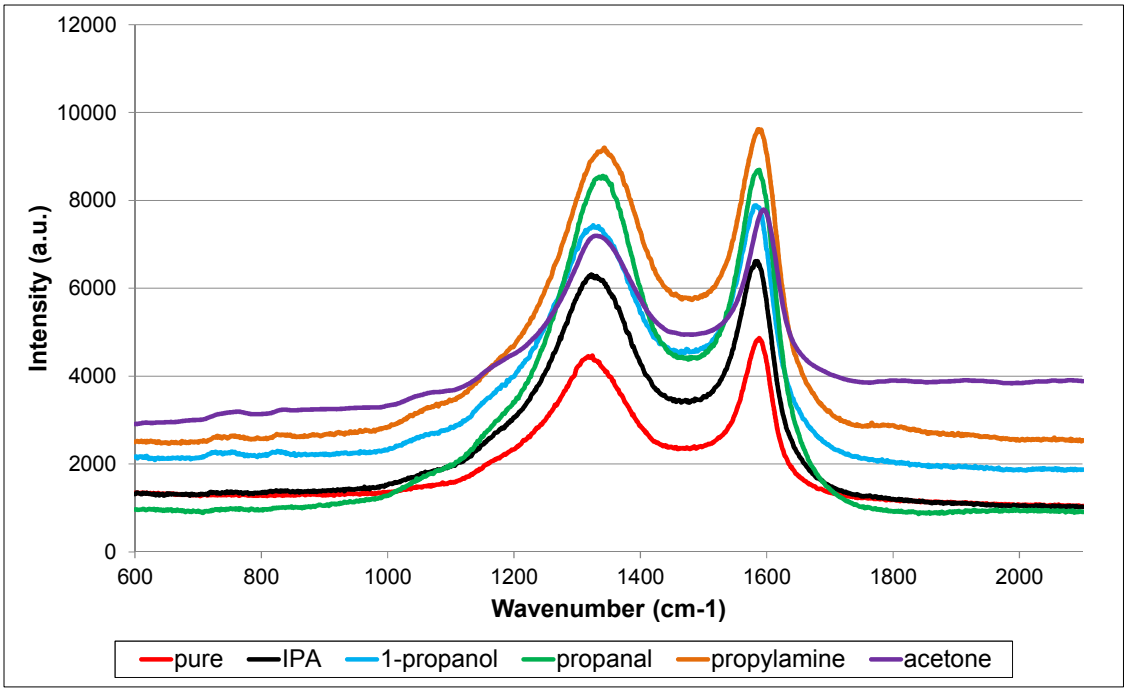

Figure 8. Raman spectra of Pt/alumina catalysts after use.

To determine the nature of coke deposition on the catalysts, the spent catalysts were analysed by TGA/DSC/MS under flow of 2% O_2/Ar gas, which is shown in Figure 9. The sole carbon containing species evolved during the TGA was carbon dioxide, which was determined by mass spectrometry. In addition to this mass, fragments with m/z

values of 2, 18, 26, 27, 28, 29, 31, 58, 59, 60 and 78 were monitored, however only trace amounts of water was detected and no prominent peaks were observed for other masses. Hence the weight loss can be assigned to the removal of carbon and the profile for the carbon dioxide evolution matches the derivative weight profile. The profiles reveal two weight loss events, at 900 – 960 K and 800 – 825 K, for all the catalysts except the one exposed to the feed with the acetone impurity, which only exhibits one clear weight loss at 954 K. The weight loss is reported in table 4.

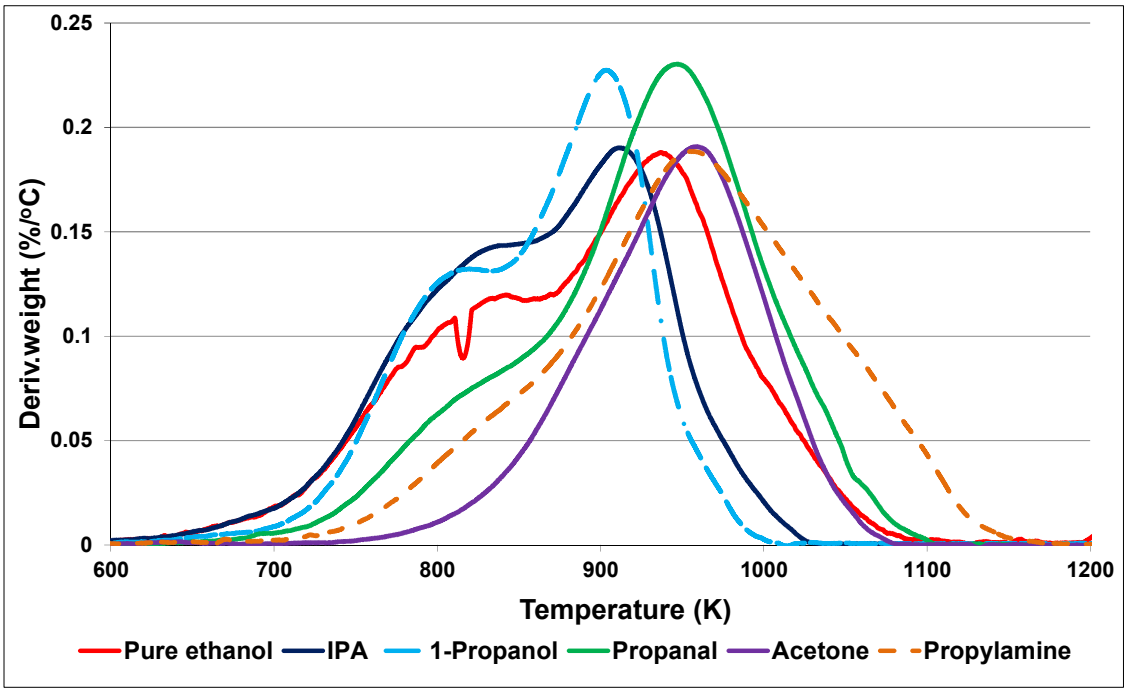

Figure 9. TGA analysis of spent Pt/alumina ESR catalysts in 2 % O_2/Ar. Weight loss represents loss of carbon dioxide.

The BET surface areas of the catalysts after 100 h TOS are reported in table 4. There is significant loss in area and pore volume for all the catalysts, although samples which had been subject to feed containing propanal and propylamine showed the lowest values.

Table 4. BET surface area, % weight loss and Raman band ratios over Pt/Al_2O_3 catalyst for different impurity reactions

Impurity	BET Surface area (m^2/g)	Pore volume (cm^3/g)	Weight loss in TPO (%)	(I_D/I_G)
Reduced@600	100	0.46	-	-
No impurity	41	0.09	37	0.92
IPA	53	0.12	34	0.94
1-propanol	64	0.15	32	0.94
Propanal	31	0.07	38	0.98
Propylamine	34	0.07	37	0.95
Acetone	57	0.17	25	0.91

To study the catalyst morphology, all of the spent Pt/alumina catalysts were analysed by SEM (Fig. 10). The SEM images show that no carbon nanotubes (CNTs) were observed in the pure ethanol reaction but the catalysts that had seen 1-propanol, acetone and propanal a few small CNTs were observed.

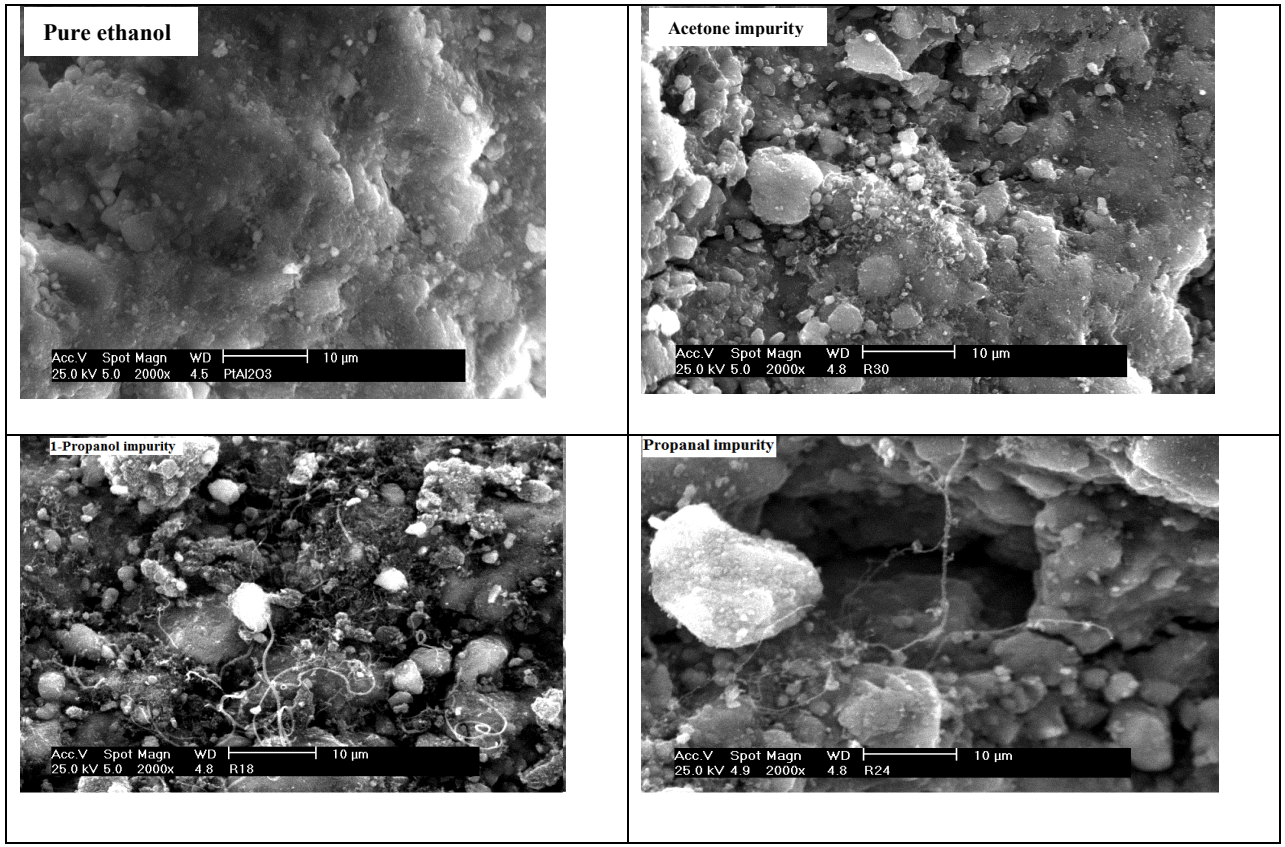

Figure 10. SEM images for post reaction Pt/Al_2O_3 catalysts

4. Discussion

In previous papers we investigated the effect of temperature on the ESR reaction over Ru/alumina [18] and Rh/alumina and Pt/alumina [1] and then the effect of impurities on the ESR reaction over Ru/alumina [17]. Ruthenium had been chosen as it had shown some resistance to poisoning [20] however we found that many of the impurities had significant effects on the ethanol conversion and dry gas selectivity. To determine whether these effects were general or specific to ruthenium we have studied rhodium and platinum and shown that platinum behaves in a similar manner to ruthenium but rhodium shows different behaviour. The hydrogen yield for the three catalysts is shown in table 5 (Ru/alumina data taken from ref. 17) and as would be expected shows that rhodium is the most effective catalyst for steam reforming to produce hydrogen. Our data for all three catalysts also concurs with Epron and co-workers' data [21] for ESR over $Rh/MgAl_2O_4$ where they found that a feed with an amine impurity gave the highest hydrogen yield and that a feed with an aldehyde yield gave the second highest yield.

Table 5. Hydrogen yield ($mol.mol^{-1}$) at 100 h TOS over the catalysts at 773 K

	Yield ($mol.mol^{-1}$)					
	Pure ethanol	IPA	1-Propanol	Propanal	Propylamine	Acetone
Rh/alumina	2.74	2.72	2.45	2.79	3.26	2.62
Pt/alumina	2.28	2.18	2.32	3.11	3.13	2.72
Ru/alumina	2.10	2.06	2.17	3.14	3.18	2.66

However even though each of the catalysts appears to behave in a similar manner we believe that the underlying mechanism is not common to all three.

4.1. Rh/alumina.

In the initial stage of the experiments (< 24 h) all the impurities resulted in a higher conversion than the pure ethanol, however by 100 h TOS the reactions with 1-propanol and IPA added had deactivated significantly while the propylamine system was now lower in activity than the pure ethanol. At 773 K over the Rh/alumina with pure ethanol the non-condensed gas phase product distribution can be described by the following equations:

$18C_2H_5OH \rightarrow 18C_2H_4 + 18H_2O$

$2C_2H_4 + 2H_2 \rightarrow 2C_2H_6$

$9C_2H_5OH + 9H_2O \rightarrow 18CO + 36H_2$

$8CO + 8H_2O \rightarrow 8CO_2 + 8H_2$

$6CO + 18H_2 \rightarrow 6CH_4 + 6H_2O$

Overall:

$27C_2H_5OH + 11H_2O \rightarrow 14H_2 + 8CO_2 + 4CO + 6CH_4 + 16C_2H_4 + 2C_2H_6 + 18H_2O$

(Reactions that generate products that were condensed as liquids are considered below. Similarly intermediates which are produced and destroyed in the formation of the gas phase products, e.g. acetaldehyde, are not shown.)

As we have outlined previously this underestimates the hydrogen yield as it takes no account of hydrogen produced during carbon laydown [17-19]. Nevertheless it does give a correct carbon and oxygen balance. From this analysis it is clear that the ratio of ethanol reactions is 2:1 ethanol dehydration:ethanol steam reforming. When both IPA and 1-propanol are added as impurities a similar behaviour pattern is observed with ethanol dehydration to ethene and water being the most prolific ethanol reaction. However even though the equilibrium position favours ethane (~ 95 %), very little ethene is hydrogenated to ethane. This behaviour was seen previously with Rh/alumina [19] and was understood in the context of the catalyst being effectively poisoned for ethene hydrogenation by the presence of carbon monoxide. The rapid deactivation observed when using these impurities (IPA and 1-propanol) can be ascribed to the formation of the respective alkenes by dehydration, similar to that found with ethanol. Note that there is no significant increase in the amount of carbon deposited or the nature of the carbon. When propylamine, propanal and acetone are the impurities, ethanol dehydration is severely inhibited with very little ethene produced (typically < 1 % of that produced from the pure ethanol). Note that ethanol dehydration does not take place over the support in the absence of metal [18]. So for the propanal impurity system the gas phase product distribution can be described by the following equations:

$27.5C_2H_5OH + 27.5H_2O \rightarrow 110H_2 + 55CO$

$19CO + 19H_2O \rightarrow 19CO_2 + 19H_2$

$29CO + 87H_2 \rightarrow 29CH_4 + 29H_2O$

Overall:

$27.5C_2H_5OH + 17.5H_2O \rightarrow 42H_2 + 19CO_2 + 7CO + 29CH_4$

To compare this with the reaction using pure ethanol, the ethanol dehydration reaction can be removed from the analysis and then the amount of ethanol reacting is normalised. When we do this we get the following for pure ethanol:

$27C_2H_5OH + 33H_2O \rightarrow 78H_2 + 24CO_2 + 12CO + 18CH_4$

Immediately it can be seen that the amount of methane is much less in the pure ethanol reaction while the carbon monoxide, carbon dioxide and hydrogen amounts are higher, indicating less carbon oxide hydrogenation is taking place. The equilibrium values under the conditions used are 27 % hydrogen, 48 % methane, 24 % carbon dioxide and 1 % carbon monoxide. This gives a $(CO_2 + CO):CH_4$ ratio of ~0.5. The $(CO_2 + CO):CH_4$ ratio for the eluant gas from the reaction which has propanal as an impurity is 0.89. Indeed performing a similar analysis with all the experiments, gives a ratio of 0.85 for the reaction with propylamine, 0.87 for the reaction with acetone but for the reaction containing 1-propanol a ratio of 2.4 was obtained, while a ratio of 2.8 was obtained from the reaction that had IPA as the impurity, the pure ethanol experiment gave a ratio of 1.9. These results suggest that the reactions containing propanal, propylamine and acetone are closer to equilibrium than those where an alcohol was added. Each alcohol can dehydrate to form an alkene which is a main source of catalyst deactivation [21, 22], therefore it would appear that the alcohols deactivate the system whereas the propanal, propylamine and acetone reduce the deactivation by inhibiting the formation of alkene. Typically acid sites would catalyse dehydration but metal sites have also been shown to catalyse this reaction. There would be a clear link with the basicity of the impurities and the inhibition of alcohol dehydration if acid sites were responsible, it is less clear if a metal site is

responsible, although amines have been identified as poisons for precious metal systems [23].

When the products that have been condensed as liquids are considered, the different effects of the impurities are clearly seen. The yield of acetaldehyde decreases with TOS for the pure ethanol reaction and similar, if less well defined behaviour, is seen with reactions with IPA and 1-propanol as the added impurities. In contrast reactions where propylamine or acetone was added show a growth of acetaldehyde with TOS: the reaction with propanal shows behaviour that has aspects of both groups. These results are markedly different from other reports in the literature, where generally the yield of acetaldehyde is low and the effect of any impurity on acetaldehyde yield is negligible [21]. However the difference in behaviour reveals a difference in the mechanism of catalyst deactivation. Previous studies have shown [24, 25] that in ethanol steam reforming, ethanol can dehydrogenate to form acetaldehyde and then acetaldehyde can further react to give carbon monoxide and methane or be steam reformed:

$C_2H_5OH \rightarrow CH_3CHO + H_2$

$CH_3CHO \rightarrow CH_4 + CO$

$CH_3CHO + H_2O \rightarrow 3H_2 + 2CO$

hence when pure ethanol is the feed or another alcohol is present, it is the dehydrogenation reaction that is reduced in rate, however when acetone or propylamine are present as impurities it is decomposition of acetaldehyde and/or the steam reforming that is reduced in rate. This suggests two separate sites for these reactions and that they are deactivated in different ways depending upon the impurity.

As expected there was significant carbon deposition during the steam reforming of ethanol with and without impurities being present. TPO of the deposit revealed two carbon combustion events at ~ 860 – 920 K and ~950 – 980 K. From the weight loss it can be calculated that the amount of carbon deposited on the surface relative to the amount of carbon passed over the catalyst during the experiment is < 0.1 %. Can et al. [26] found four different types of coke over a Rh/Al_2O_3 catalyst after use in ESR at 673 K for 8 h.. Type I (583 K) they assigned to coke deposited on the metal, type II (653 K) to coke deposited around the metal–support interface, type III (793 K) to carbon deposited on the support, while type IV (968 K) was assigned to a graphite phase generated by the thermal decomposition of ethanol. Our TPO profiles do not show a similar profile, which may be due to the temperature of reaction and/or the time on stream. We have previously shown [18, 19] that, after use in ESR, the alumina gives a TPO evolution at 985 K that can be assigned to graphitic carbon formed through ethanol decomposition. However over the alumina the extent of carbon deposition was much smaller than that observed over the catalysts. Nevertheless the carbon dioxide evolution at ~950 – 980 K can be associated with graphitic carbon on the support. Hence the weight loss/carbon dioxide evolution at ~ 860 – 920 K can be assigned to carbon associated with the metal. Note that the amount of carbon deposition is essentially the same, as is the nature, yet the deactivation profiles are considerably different. This suggests that the majority of the carbon deposited has no effect on catalyst activity and that only a small proportion affects catalyst deactivation.

4.2. Pt/alumina.

At first sight the behaviour of the Pt/alumina catalyst mirrors that of the Rh/alumina. However on closer inspection there are subtle differences that suggest a different interpretation. At 773 K over Pt/alumina with pure ethanol the gas phase product distribution can be described by the following equations:

$12C_2H_5OH \rightarrow 12C_2H_4 + 12H_2O$

$2C_2H_4 + 2H_2 \rightarrow 2C_2H_6$

$4C_2H_5OH + 4H_2O \rightarrow 8CO + 16H_2$

$4CO + 4H_2O \rightarrow 4CO_2 + 4H_2$

$3CO + 9H_2 \rightarrow 3CH_4 + 3H_2O$

Overall:

$16C_2H_5OH + 5H_2O \rightarrow 23H_2 + 4CO_2 + CO + 3CH_4 + 10C_2H_4 + 2C_2H_6 + 12H_2O$

This gives a $(CO + CO_2):CH_4$ ratio of 1.7 and the ratios obtained when IPA and 1-propanol are used as impurities are 1.6 and 1.7 respectively. However when the reactions that contain propanal, acetone and propylamine are examined the $(CO + CO_2):CH_4$ ratio is 1:1, which is the same as that found over the alumina support and is indicative of ethanol decomposition rather than steam reforming. Figure 11 shows the dry gas selectivities for the Pt/alumina reactions and for the alumina support, where the similarities in product distribution between the alumina support and the reactions involving acetone, propylamine and propanal is clear. This behaviour was also seen with Ru/alumina [17]

Generally the TGA profiles of the deposited carbon were similar for each reaction over the Ru/alumina [17] and Rh/alumina catalysts (Fig. 4). However this is not the case with Pt/alumina (Fig. 9). Carbon laydown in systems such as these can come from a variety of sources such as the Boudouard reaction, ethene cracking, and methane cracking [9]. However it is unlikely that the Boudouard reaction ($2CO \rightarrow CO_2 + C$) is a major contributor to carbon deposition given the CO_2:CO ratio in the product gas and the high water partial pressure, which can remove active carbon e.g.

$2CO \rightarrow CO_2 + C$

$H_2O + C \rightarrow CO + H_2$

overall this gives the WGS reaction, where the carbon is a reactive intermediate. In contrast ethene cracking is much more likely especially over the support [27] and would contribute to the formation of CNTs over the metal component [28]. This interpretation would be in agreement with a thermodynamic study of carbon deposition during ethanol steam reforming [29]. As well as these routes the impurity itself can also contribute to the carbon deposition. For example acetone has been shown to polymerize under steam reforming conditions resulting in catalyst deactivation [30]. Also ethanol has been shown to be a suitable feedstock for the production of single-walled carbon nanotubes (SWCNT) at 773 K [31] probably via the formation of ethene [28]. The carbon evolution at ~800 – 825 K is very clear with pure ethanol and tests using IPA and 1-propanol as impurities but when propanal is the impurity the evolution is reduced and further reduced with propylamine. When acetone is the impurity there is no evolution at low temperature, there is only a single evolution at ~975 K. This single evolution is typical of that found for the alumina support in the absence of metal [18]. This suggests that the low

temperature evolution is related to carbon formed on/by the metal function, therefore either there is no deactivation of the metal (the acetone inhibits carbon deposition on the metal) or the metal is rapidly deactivated and all the chemistry takes place on the support. The product distribution suggests that the latter is the correct interpretation.

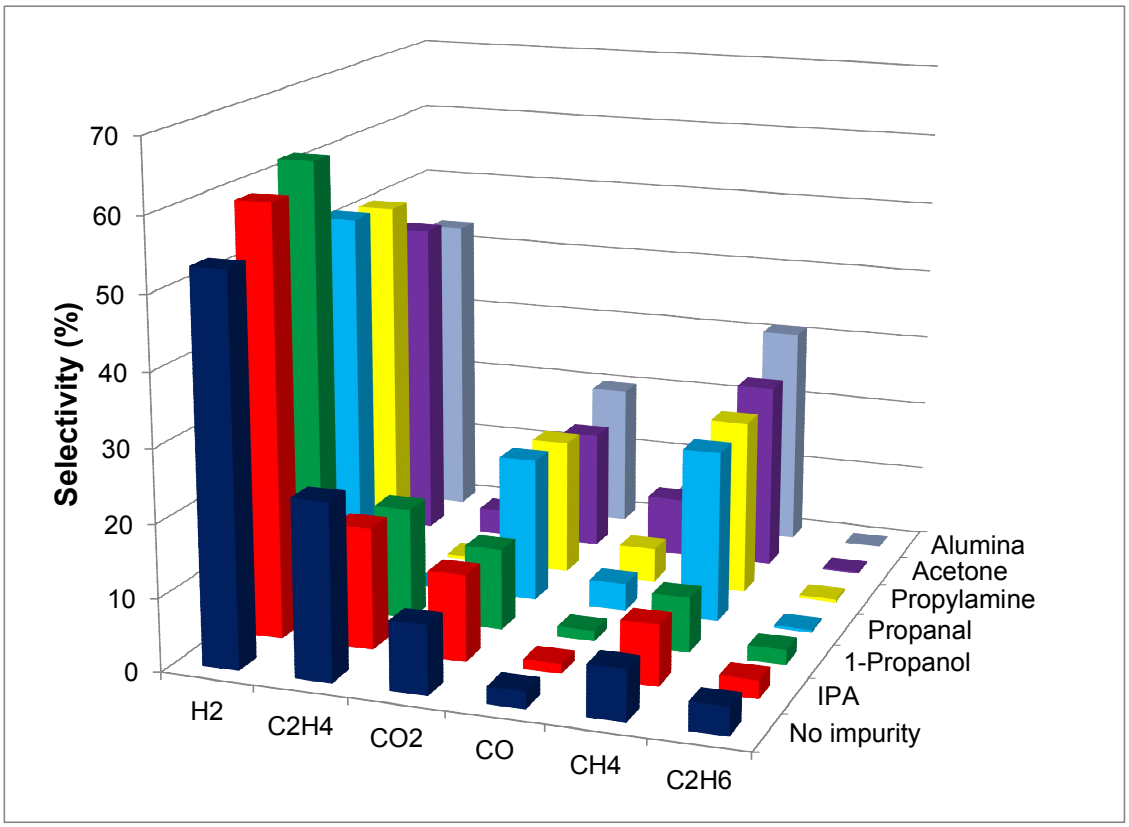

Figure 11. Comparison of dry gas selectivities for ESR over the Pt/alumina catalyst and the alumina support.

5. Conclusions

The presence of 1mol. % organic impurities in the water/ethanol mixture significantly increases or decreases the conversion of ethanol over the Pt/Al_2O_3 and Rh/Al_2O_3 catalysts

depending upon the impurity added. It was concluded that both the alcoholic (IPA and 1-propanol) impurities deactivated the catalysts severely towards the conversion of ethanol whilst the propanal, propylamine and acetone impurities enhanced the conversion of ethanol and delayed the deactivation with respect to the pure ethanol reaction. However this hides significant differences between the catalysts and the effect of the impurities. It has long been known that rhodium is the most of the group VIII elements for methane steam reforming, while platinum is one of the least active [32, 33]. The reason for this relates to the C and O adsorption energies over the metals [34]. It is likely that as the formation of carbon monoxide is the key kinetic step [34] a similar order would be obtained for ethanol steam reforming, especially as the dehydrogenation to acetaldehyde followed by reaction of methane is considered one of the main reaction routes for ethanol steam reforming. Over the Pt/alumina catalyst the data indicated that when propanal, propylamine and acetone were present as impurities the steam reforming reaction was rapidly poisoned and the high conversion related to ethanol decomposition resulting in lower hydrogen yields and higher methane yields. The impurities also caused a change in the nature and extent of carbon laydown over Pt/alumina, with the carbon deposit associated with the metal decreasing in the order IPA > 1-propanol > pure ethanol > propanal > propylamine > acetone. In contrast over the Rh/alumina the steam reforming reaction was maintained and the carbon deposition showed no trend relative to the impurities. The gaseous products were closer to thermodynamic equilibrium over the Rh/alumina when propanal, propylamine and acetone impurities were present, indicating a higher reactivity for subsequent reactions after the initial ethanol conversion.

Acknowledgements

The authors are grateful to Kohat University of Science and Technology Kohat, Pakistan for the support of a studentship to one of us (MB).

References

[1] H. Balat, E. Kirtay, Int. J. Hydrogen Energy, 35 (2010) 7416-7426.

[2] A. Uihlein, D. Magagna, Renewable and Sustainable Energy Reviews 58 (2016) 1070–1081.

[3] D. Shekhawat, J.J. Spivey, D. Berry Fuel Cells: Technology for Fuel Cell Processing, Elsevier, Oxford, 2011.

[4] O. Z. Sharaf, M. F. Orhan, Renewable and Sustainable Energy Reviews 32 (2014) 810–853.

[5] R.C. Cerritos, R.F. Ramirez, A.F. A. Alvarado, J.M.M. Rosales, T.V. García, I.R.G. Esquivel, Ind. Eng. Chem. Res., 50 (2011) 2576-2584.

[6] I.A.C. Ramos, T. Montini, B. Lorenzut, H. Troiani, F.C. Gennari, M. Graziani, P. Fornasiero, Catal. Today, 180 (2012) 180, 96-104.

[7] I. Dincer, C. Acar, Int. J.Hydrogen Energy 40 (2015) 11094-11111.

[8] A.C. Furtado, C.G. Alonso, M.P. Cantão, N.R.C. Fernandes-Machado, Int. J. Hydrogen Energy, 34 (2009) 7189-7196.

[9] N. Bion, F. Epron, D. Duprez. Catalysis, The Royal Society of Chemistry, 2010, pp. 1-55.

[10] A. Le-Valant, F. Can, N. Bion, D. Duprez, F. Epron, Int. J. Hydrogen Energy, 35 (2010) 5015-5020.

[11] A. Bshish, Z. Yakoob, B. Narayanan, R. Ramakrishnan, A. Ebshish, Chem. Pap., 65 (2010) 251-266.

[12] M. Benito, J.L. Sanz, R. Isabel, R. Padilla, R. Arjona, L. Daza, Journal of Power Sources, 151 (2005) 11-17.

[13] L.C. Chen, S.D. Lin, Appl. Catal. B, 106 (2011) 639-649.

[14] H. Habe, T. Shinbo, T. Yamamoto, S. Sato, H. Shimada, K. Sakaki, J. Japan Petrol. Inst 56 (2013) 414-422.

[15] A.J. Akande, R.O. Idem, A.K. Dalai, Appl. Catal. A, 287 (2005) 159-175.

[16] A. Le-Valant, A. Garron, N. Bion, D. Duprez, F. Epron, Int. J. Hydrogen Energy, 36 (2011) 311-318.

[17] M. Bilal, S.D. Jackson, Catal. Sci. Technol., 4 (2014) 4055-4064

[18] M. Bilal, S.D. Jackson, Catal. Sci. Technol., 2 (2012) 2043-2051

[19] M.Bilal, S.D. Jackson, Catal. Sci. Technol., 3 (2013) 754-766

[20] J. Rass-Hansen, R. Johansson, M. Moller, C.H. Christensen, Int. J. Hydrogen Energy, 33 (2008) 4547-4554.

[21] A. Le Valant, A. Garron, N. Bion, F. Epron, D. Duprez, Catal. Today, 138 (2008) 169-174

[22] S. Cavallaro, Energy & Fuels, 14 (2000) 1195-1199

[23] K.F. Graham, K.T. Hindle, S.D. Jackson, D.J.M. Williams, S. Wuttke, Top. Catal., 53 (2010) 1121-1125

[24] J. Raskó, A. Hancz, A. Erdohelyi, Appl. Catal. A, 269 (2004) 13-25

[25] F. Aupretre, C. Descorme, D. Duprez, D. Casanave, D. Uzio, J. Catal., 233 (2005) 464-477

[26] F. Can, A. Le Valant, N. Bion, F. Epron, D. Duprez, J. Phys. Chem. C, 112 (2008) 14145-14153

[27] P. Osorio-Vargas, C. H. Campos, R. M. Navarro, J. L.G. Fierro, P. Reyes, Appl. Catal. A 505 (2015) 159–172

[28] S. Takenaka, T. Iguchi, E. Tanabe, H. Matsune, M. Kishida, Carbon 47 (2009) 1251–1257

[29] A. L. da Silva, C. de F. Malfatti, I. L. Muller, Int. J. Hydrogen Energy 34 (2009) 4321–4330

[30] X. Hu, G. Lu, Appl. Catal. B 88 (2009) 376–385.

[31] N. Fukuoka, Y. Mizutani, S. Naritsuka, T. Maruyama, S. Iijima, Jpn. J. Appl. Physics 51 (2012) 06FD23

[32] J. R. Rostrup-Nielsen, J. Catal. 31 (1973) 173-199

[33] D. Qin, J. Lapszwicz, Catal. Today 21 (1994) 551-560

[34] G. Jones, J. G. Jakobsen, S. S. Shim, J. Kleis, M. P. Andersson, J. Rossmeisl, F. Abild-Pedersen, T. Bligaard, S. Helveg, B. Hinnemann, J. R. Rostrup-Nielsen, I. Chorkendorff, J. Sehested, J. K. Nørskov, J. Catal. 259 (2008) 147–160